Pressure and Temperature Dependence of the Longitudinal Proton and Deuteron Relaxation Rates in NH_3 and ND_3

H. Hauer, E. Lang, and H.-D. Lüdemann

Institut für Biophysik und Physikalische Biochemie, Universität Regensburg, Postfach 397, D-8400 Regensburg

Flüssigkeiten / Hohe Drücke / Magnetische Kernresonanz / Transporterscheinungen

The molecular mobility of liquid ammonia is derived from the determination of the longitudinal relaxation times of the protons and deuterons. The experiments were performed in the temperature interval between the melting pressure curve and 467 K for NH_3 and to 351 K for ND_3 at pressures up to 250 MPa. At temperatures below ~350 K the molecular mobility can be described by the isotropic small-step diffusion model. The activation energies at constant pressure are derived for the rotatoric diffusion to $7.0 \pm 0.5\,kJ \cdot mol^{-1}$ and for the translatoric diffusion to $6 \pm 1\,kJ \cdot mol^{-1}$ from the temperature dependence of the relaxation rates. In addition the activation energy at constant volume for the rotatoric diffusion has been determined to $5.7 \pm 0.5\,kJ \cdot mol^{-1}$. The isotherms for all relaxation rates are linear in a $\log(1/T_1)$ versus $1/T$ plot, yielding $\Delta V^{\neq}_{intra} = 2.5 \pm 0.6\,cm^3 \cdot mol^{-1}$ and $\Delta V^{\neq}_{inter} = 5 \pm 1\,cm^3 \cdot mol^{-1}$.

Die molekulare Beweglichkeit des flüssigen Ammoniaks wurde mit Hilfe longitudinaler Relaxationszeitmessungen der Protonen und Deuteronen untersucht. Die Messungen wurden im Temperaturbereich zwischen der Schmelzdruckkurve und 467 K für NH_3 bzw. 351 K für ND_3 bei Drücken bis 250 MPa vorgenommen. Bei Temperaturen $\lesssim$350 K läßt sich die molekulare Beweglichkeit durch ein isotropes small-step Diffusionsmodell beschreiben. Aus der Temperaturabhängigkeit der Relaxationsraten wurden die Aktivierungsenergien bei konstantem Druck für die rotatorische Diffusion zu $7{,}0 \pm 0{,}5\,kJ \cdot mol^{-1}$ und für die translatorische Diffusion zu $6 \pm 1\,kJ \cdot mol^{-1}$ bestimmt. Für die rotatorische Diffusion wurde die Aktivierungsenergie bei konstantem Volumen zu $5{,}7 \pm 0{,}5\,kJ \cdot mol^{-1}$ errechnet. Die Isothermen für alle Relaxationsraten verlaufen in einer $\log 1/T_1$ gegen $1/T$ Darstellung linear. ($\Delta V^{\neq}_{intra} = 2{,}5 \pm 0.6\,cm^3 \cdot mol^{-1}$, $\Delta V^{\neq}_{inter} = 5 \pm 1\,cm^3 \cdot mol^{-1}$).

Introduction

The hydrides of nitrogen, oxygen, and fluorine form liquids with rather unique structures. The physical properties of these liquids are normally explained by the ability of these three hydrides to participate in hydrogen bonding with their hydrogen atoms as well as with the lone electron pairs. The pronounced hydrogen bonding in liquid water is well established [1]. As derived from small angle X-ray and neutron scattering liquid ammonia however does possess a significantly different radial distribution function with approximately 12 next neighbours [2] as compared to the 4–5 next neighbours of water.

Though liquid ammonia has been the subject of several investigations, it is still the subject of discussion whether the dynamic properties of this liquid reveal significant hydrogen bonding, and different authors have derived from their data pronounced hydrogen bonding [3, 4] as well as no contribution at all from this interaction [5, 6].

As well known, NMR presents a powerful tool for the study of molecular motions in liquids. Valuable information can be gained from the temperature- and pressure dependence of the spin-lattice relaxation times. Previous work has investigated the temperature dependence of the relaxation times of H [7], ^{14}N [3, 8] and ^{15}N [4] in NH_3 and D [8, 9], ^{14}N [8], and ^{15}N [4] in liquid ND_3. In this paper the pressure dependence

Ber. Bunsenges. Phys. Chem. *83*, 1262–1269 (1979) – © Verlag Chemie, D-6940 Weinheim, 1979.
0005-9021/79/1212-1262 $ 02.50/0

of the relaxation rates of H in NH_3 and D in ND_3 is presented. In the PT-region studied, the relaxation of the deuterons in ND_3 is completely determined by the quadrupole relaxation mechanism. In the low temperature range the proton relaxation is dominated by the dipole-dipole mechanism, at higher temperatures the spin-rotation mechanism contributes significantly to the observed relaxation rate.

Experimental

The deuteron and proton longitudinal relaxation times T_1 were obtained on a Varian XL 100-15 Ft NMR spectrometer interfaced to a 16 K Varian 620L-100 computer with disk accessory by a t_1-90°-t_2-180°-t_1-90° pulse sequence. The observe frequency on this instrument is 100.1 MHz for protons and 15.4 MHz for deuterons. A modified variable temperature accessory of this spectrometer was used in the experiments. The temperatures were determined to ±0.5 K with a metal sheathed miniature chromel-alumel thermocouple. Deuteroammonia (99 % deuterated) was purchased from Sharp and Dohme, München.

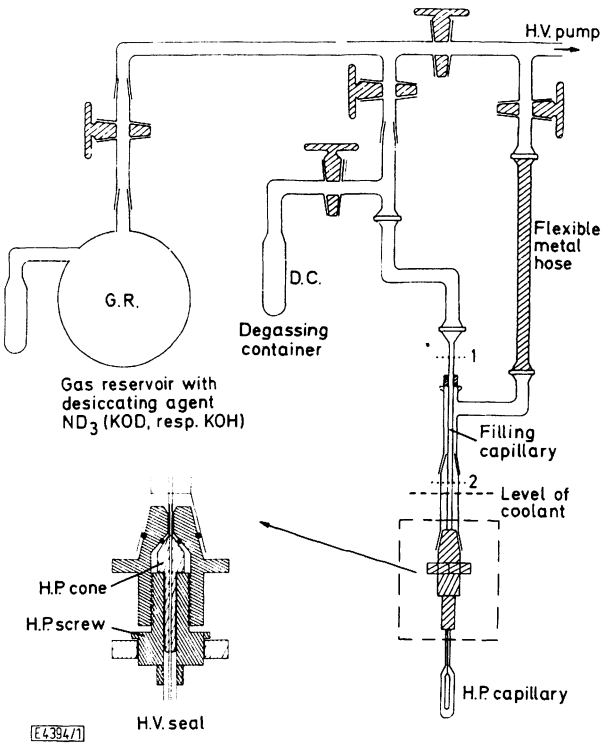

Fig. 1
High vacuum apparatus for the filling of oxygen free low boiling substances into the high pressure capillaries. (For functional details see text)

The high pressure equipment used has been described previously [10]. Oxygen-free dry ammonia was prepared in the high vacuum apparatus described in Fig. 1. A proper quantity of dried ammonia was condensed from the reservoir into the degassing container (D.C.) by cooling this container with acetone/carbondioxyde mixtures. The sample was thoroughly degassed by at least five freeze-pumpe-thaw cycles to a final pressure of $7 \cdot 10^{-3}$ Pa. Freezing was accomplished by immersing the container (D.C.) into liquid nitrogen, the melting of the ammonia was done in acetone/carbondioxyde mixtures. After degassing of the ammonia the high pressure capillary was immersed in a methylcyclohexane bath to the level indicated in Fig. 1 and cooled to 205 K. All connections to the high vacuum line were shut off and the ammonia in the degassing container allowd to warm up. After sufficient ammonia had condensed into the high pressure capillary, the filling glass capillary was flame sealed at position 1. All glass parts and the high vacuum seal (H.V.S.) wee removed under continuous cooling from the high pressure capillary and the filling capillary was resealed at position 2. The precooled copper beryllium cell was screwed onto the high pressur cell, while the assembly remained in the cold methylcyclohexane. The whole assembly was connected to the pressure generating equipment and a pressure of 20 MPa was applied. Afterwads the whole assembly was removed from the cold methylcyclohexane bath.

This elaborate procedure was necessary for two reasons:

1. The Teflon shrink hose, which separates the liquid under study from the pressure generating liquid is not sufficiently vacuum tight to permit the filling of oxygen-free liquid.
2. The low boiling point of ammonia demands that all filling and sealing operations are done at temperatures well below 230 K.

As controlled by repeated T_1-measurements under identical conditions, the ammonia in properly filled and assembled cells remains free of any contamination for several months.

Theory

The main relaxation mechanisms for proton and deuteron relaxation are the direct dipole-dipole interaction, the spin-rotation interaction and the quadrupole interaction.

Dipole-Dipole and Spin-Rotation Relaxation for Protons

The dipole-dipole interaction contains two contributions due to the interaction of the nuclei within the same molecule and due to nuclei on different molecules. The intramolecular relaxation rate $(1/T_1)_{intra}$ is due to changes in the orientation of the vector r_{12} connecting two nuclei within the same molecule, whereas the intermolecular relaxation rate $(1/T_1)_{inter}$ is due to changes in length and orientation of r_{12} between nuclei on different molecules. For a liquid consisting of isotropically reorienting molecules the intramolecular reaxation rate is under extreme narrowing conditions given by [1–14]

$$\left(\frac{1}{T_1}\right)_{intra} = \frac{3}{2}\sum_{i>j}\frac{\gamma^4\hbar^2}{r_{ij}^6}\tau_{\theta,\mathrm{eff}}^{(2)} \tag{1}$$

where the sum runs over all spin pairs that contribute to the relaxation of a single spin and $\tau_{\theta,\mathrm{eff}}^{(2)}$ is the zero frequency Fourier transform of the corresponding auto-correlation function. For a symmetric top $\tau_{\theta,\mathrm{eff}}^{(2)}$ is given in the Refs. [13, 15].

The intermolecular dipolar contribution is generally calculated assuming modulation of the dipole-dipole interaction by translational diffusion only. This gives [11]

$$\left(\frac{1}{T_1}\right)_{inter} = \frac{6\pi^2}{5}\hbar^2\gamma^4\frac{N\cdot\eta}{T}. \tag{2}$$

Various modifications of this equation have been given [16, 20]. In the following only the proportionality between $(1/T_1)_{inter}$ and $(\rho\cdot\eta)/T$ will be used.

The spin-rotation interaction is caused through a magnetic field produced by rotations of the charge distribution in the vicinity of a given nucleus [21]. The relaxation rate caused by this mechanism is usually given by [12, 21].

$$\left(\frac{1}{T_1}\right)_{SR} = \frac{2kT}{3\hbar^2}\tau_J\sum_{i,j}I_jC_{ij}^2. \tag{3}$$

In this equation it is assumed that no correlation exists between the orientation and the angular momentum. In the axis system of the moment of inertia tensor the latter is equivalent to the angular velocity correlation function, which is the actual quantity of interest in liquids. Further it is assumed that $\tau_{Jj} = \tau_J$. The spin-rotation coupling tensor c for the protons in NH_3 contains non-diagonal

elements in the principal inertial axis system [3]. Its elements can be obtained from microwave data [23, 24].

Quadrupole Interaction

The quadrupole relaxation rate is in the extreme narrowing limit and with an axially symmetric field gradient tensor given through the relation

$$\left(\frac{1}{T_1}\right)_Q = \frac{3}{8}\left(\frac{e^2qQ}{h}\right)^2 \tau^{(2)}_{\theta,\mathrm{eff}}. \tag{4}$$

The correlation time $\tau^{(2)}_{\theta,\mathrm{eff}}$ is given by [15, 16] with θ the angle between the symmetry axis of the molecule and the symmetry axis of the field gradient tensor.

Separation of the Different Contributions of the Proton Relaxation Times T_1

Provided the quadrupole coupling constant QCC) is known for a given molecule in the liquid, the reorientational correlation time $\tau^{(2)}_{\theta,\mathrm{eff}}$ is directly determined from the experimental relaxation rate. Atkins et al. [8] showed for the case of liquid ammonia that the correlation times $\tau^{(2)}_{\theta,\mathrm{eff}}$ transform under isotopic substitution as

$$\frac{\tau_\theta(\mathrm{NH_3})}{\tau_\theta(\mathrm{ND_3})} = \left(\frac{I(\mathrm{NH_3})}{I(\mathrm{ND_3})}\right)^{1/2} \tag{5}$$

I = moment of inertia

Thus one can get directly the correlation time for the intramolecular dipolar relaxation rate in NH_3 from the measured deuteron relaxation times of ND_3. In the rotational diffusion limit the reorientational correlation time $\tau^{(2)}_{\theta,\mathrm{eff}}$ and the angular momentum correlation time τ_J are related by [15, 25]

$$\tau^{(2)}_{\theta,\mathrm{eff}} \cdot \tau_J = \frac{I_\perp}{6kT} \cdot f_2(\theta,\alpha), \qquad \alpha = \frac{I_\perp}{I_\parallel},$$
$$f_2(\theta,\alpha) = \frac{(3\cos^2\theta - 1)^2}{4} + \frac{18\sin^2\theta\cos^2\theta}{5+\alpha} + \frac{9}{4}\frac{\sin^4\theta}{1+2\alpha} \tag{6}$$

$I_\perp$, $I_\parallel$ – component of the moment of inertia tensor.

With τ_J thus obtained, $(1/T_1)_{SR}$ can be calcuated with Eq. (5). Finally the intermolecular relaxation rate is given by

$$\left(\frac{1}{T_1}\right)_{\mathrm{inter}} = \left(\frac{1}{T_1}\right)_{\mathrm{exp}} - \left(\frac{1}{T_1}\right)_{\mathrm{intra}} - \left(\frac{1}{T_1}\right)_{\mathrm{SR}}. \tag{7}$$

Results and Discussion

Estimate of the QCC of Deuteroammonia in the Liquid State

From the determination of the longitudinal proton and deuteron relaxation times in liquid NH_3 and ND_3 Powles et al. [6, 7, 9] derived the QCC as $(e^2qQ)/h = 245 \pm 25$ kHz assuming $\tau^{DD}_\theta = \tau^Q_\theta$. Applying instead Eq. (5) proposed by Atkins et al. [8] yields: $(e^2qQ)/h = 208 \pm 21$ kHz. As can be seen from a comparison of the corresponding nitrogen-14 T_1 data of $^{14}NH_3$ and $^{14}ND_3$ [3, 8] for this nucleus the decrease of the QCC in going from the gas phase to the solid state is much smaller, and thus QCC of the liquid can be estimated with considerably higher accuracy (see Table I), the latter value is obviously the more realistic choice (see also [26]).

Relaxation Times at Saturation Pressure

The spin-lattice relaxation times at saturation pressure have been measured over the temperature range of 197 K to 311 K for NH_3 and 200 K to 310 K for ND_3. The results are shown in Fig. 2 together with the different components contributing to the observed relaxation time. The separation has been effected as described before. It should be noticed that the intermolecular relaxation rate amounts to about 60% of the measured rate and is the most effective relaxation mechanism. This conclusion is in accord with the result obtained by Powles et al. [6, 7]. However it depends strongly on the choice of the QCC. The correlation times extracted from these data are collected in Table 2. No definite decision can be made about the appropriate model of molecular motion in the case of liquid ammonia. Inspection of the correlation between τ^*_θ and τ^*_J given by Powles and Rickayzen

Table 1
Correlation times $\tau^{(2)}_{\theta,\mathrm{eff}}$ of liquid ammonia at 303 K and vapour pressure calculated from ^{14}N quadrupole relaxation times

	$^{14}N-QCC$	$\tau^{(2)}_{\theta,\mathrm{eff}}$*)	
$^{14}NH_3$	4.08 MHz (gas phase)	12.1 (fs)	11.5 (fs)
	3.47 MHz (solid state)	16.8 (fs)[a])	16.0 (fs)[b])
		↓ **)	
$^{14}ND_3$	4.08 MHz (gas phase)	16.9 (fs)	16.1 (fs)
	3.47 MHz (solid state)	23.3 (fs)	22.3 (fs)[b])

[a]) Estimated from T_1-data of Ref. [3].
[b]) Estimated from T_1-data of Ref. [8].
*) T = 303 K.
**) Transformed by application of Eq. (5) (see Atkins et al. [8]).

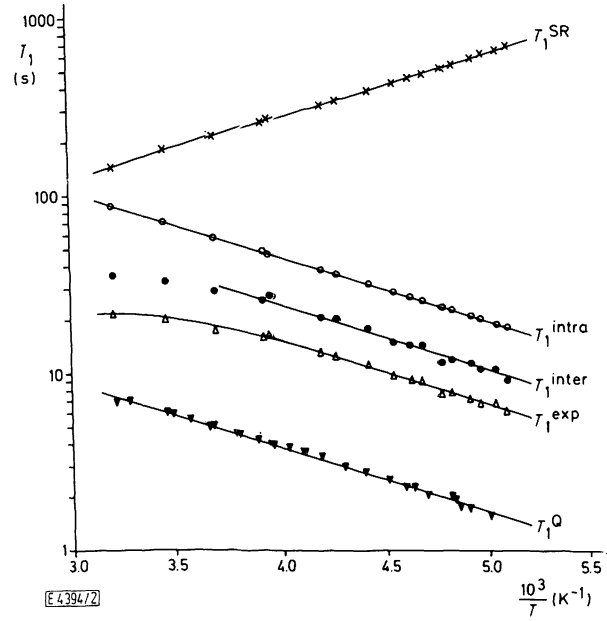

Fig. 2
Longitudinal relaxation times (T_1) of the protons in NH_3 (T_1^{exp}) and ND_3 (T_1^Q) at vapour pressure as function of the reciprocal temperature.
○ T_1^{intra} intramolecular dipole-dipole relaxation rates of the protons in NH_3.
● T_1^{inter} intermolecular dipole-dipole relaxation rates of the protons in NH_3.
× T_1^{SR} spin rotation contribution to the experimental proton T_1. Details of the separation procedure for the different contributions to the experimental proton T_1 are given in the theoretical section (Eqs. (4), (5), and (6)]

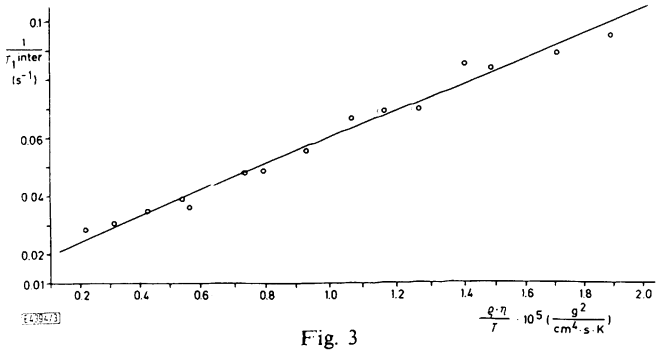

Fig. 3

Plot of $(T_1^{inter})^{-1}$ at vapour pressure vers. $(\rho \cdot \eta)/T$ according to Eq. (2). ρ = density., η = dynamic viscosity

Table 2

Correlation times $\tau_{\theta,eff}^{(2)}$ and τ_J of liquid NH_3 at vapour pressure calculated by application of Eqs. (4), (5) and (6). The experimental intermolecular relaxation rates $(1/T_1^{inter})_{exp}$ given are the difference between $(1/T_1^{intra} + 1/T_1^{SR})$ and the experimental $1/T_1$. The calculated intermolecular relaxation rates were determined with Eq. (2)

T (K)	$\tau_{\theta,eff}^{(2)}$ (fs)	τ_J (fs)	$\left(\frac{1}{T_1^{inter}}\right)_{exp}$ (s^{-1})	$\left(\frac{1}{T_1^{inter}}\right)_{calc}$ (s^{-1})
197	713	2.99	0.108	
199	683	3.09	0.094	
202	641	3.25	0.095	0.106
204	615	3.35	0.089	0.096
208	568	3.56	0.083	0.083
210	547	3.66	0.085	0.078
214	507	3.88	0.070	0.071
217	480	4.04	0.069	0.066
221	447	4.26	0.066	0.059
227	404	4.59	0.055	0.053
235	356	5.03	0.049	0.045
239	335	5.25	0.048	0.041
253	276	6.02	0.036	0.032
255	269	6.13	0.039	0.030
270	224	6.95	0.035	0.024
288	184	7.93	0.031	0.018
311	148	9.14	0.028	0.012

[27] for different models shows that almost all $\tau_{\theta,eff}^{(2)*}$ fall into the region, where the Hubbard relation holds. This renders rotational diffusional motion to be an adequate description for the dynamic behaviour of the ammonia molecules over the temperature range studied.

Fig. 3 shows the dependence of $(1/T_1)_{inter}$ on $(\rho \cdot \eta)/T$. As can be seen, the linear dependence which is predicted by Eq. (2) holds over the whole temperature range. Included in Table 2 are also the intermolecular relaxation rates calculated with Eq. (2). The agreement at low temperatures is reasonably good, the discrepancy at higher temperatures may be due to the separation procedure and to the simplicity of the underlying theoretical model. Concerning the anisotropy of the rotational motion of liquid ammonia we have estimated $\tau_\perp$ and $\tau_\parallel$ for ND_3 from the ^{14}N-T_1 data from Atkins et al. [8] and our deuteron T_1-data. At $T = 303$ K we get with QCC (^2H) = 210 kHz and QCC (^{14}N) = 3.47 MHz and the equation [12, 28].

$$\tau_{\theta,eff}^{(2)} = \tau_\perp \left[1 - \frac{3(\rho-1)}{5+\rho}\sin^2\beta\left(1 - \frac{3(\rho-1)}{2(2\rho+1)}\sin^2\beta\right)\right],$$

$$\rho = \frac{\tau_\perp}{\tau_\parallel}$$

where β is the angle between the symmetry axis of the field gradient tensor and the symmetry axis of the diffusion tensor an almost isotropic rotation, i. e. $\rho \simeq 1$.

Pressure Dependence of the Relaxation Times

The dynamic behaviour of the ammonia molecules as a function of the density has been studied up to a pressure of 250 MPa for both liquid NH_3 and ND_3. In the case of the former the temperature has been varied from 213 K to 467 K, whereas for the latter the temperature interval ranged from 213 K to 351 K. The isotherms of the spin-lattice relaxation times are shown in Figs. 4 and 5. The effective orientational correlationtimes $\tau_{\theta,eff}^{(2)}$ for ND_3 have been calculated assuming QCC(^2H) = 210 kHz; they are given in Table 3.

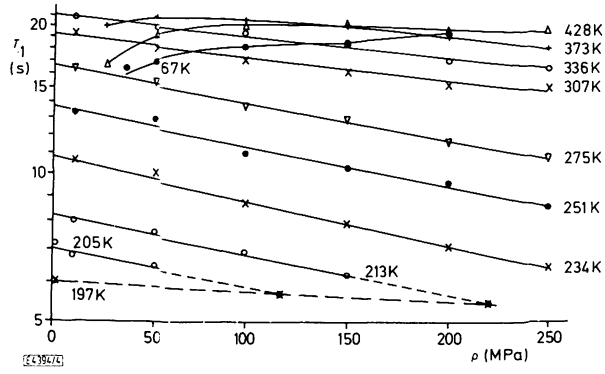

Fig. 4

Isotherms of the experimental longitudinal proton relaxation times (T_1) of liquid ammonia

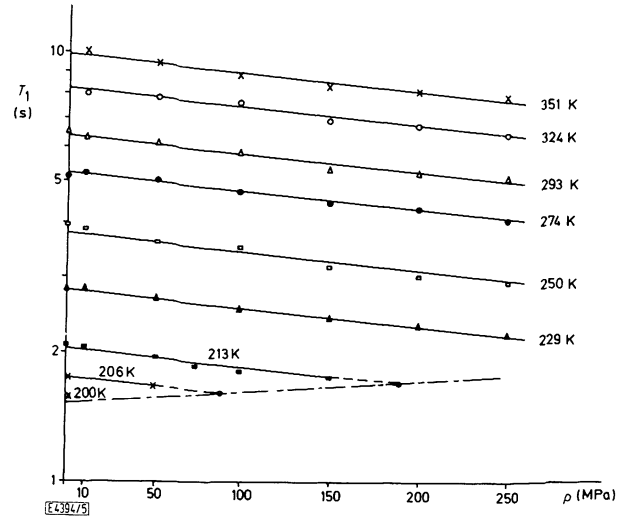

Fig. 5

Isotherms of the experimental longitudinal deuteron relaxation times (T_1) of liquid deuteroammonia

In liquid ammonia at low temperatures ($T < 350$ K) the separation procedure mentioned above was used to extract the different contributions to the total relaxation rate. The results are compiled for three pressures in Figs. 6–8. The effective orientational correlation times $\tau_{\theta,eff}^{(2)}$ for the intramolecular relaxation rate have been calculated from the $\tau_{\theta,eff}^{(2)}(ND_3)$ with Eq. (5). However, the different geometrical

Table 3
Pressure dependence of the correlation times $\tau^{(2)}_{\theta,\mathrm{eff}}$ in liquid ND_3 and τ_J in liquid NH_3

ND_3	$\tau^{(2)}_{\theta,\mathrm{eff}}$ (fs)					
T \ P	10 MPa	50 MPa	100 MPa	150 MPa	200 MPa	250 MPa
213 K	723	786	806	870	885	923
229 K	547	578	613	638	666	696
250 K	398	426	438	486	511	528
274 K	295	309	326	344	356	378
293 K	243	247	264	289	295	303
324 K	192	198	203	222	229	239
351 K	153	163	176	185	189	194

NH_3	τ_J (fs)					
T \ P	10 MPa	50 MPa	100 MPa	150 MPa	200 MPa	250 MPa
213 K	3.80	3.49	3.40	3.15	3.10	2.97
234 K	4.92	4.68	4.44	4.11	4.03	3.86
251 K	5.86	5.58	5.28	4.90	4.79	4.60
275 K	7.18	6.83	6.45	6.00	5.88	5.64
307 K	8.84	8.40	7.96	7.40	7.25	6.95
336 K	10.3	9.78	9.20	8.57	8.34	8.07

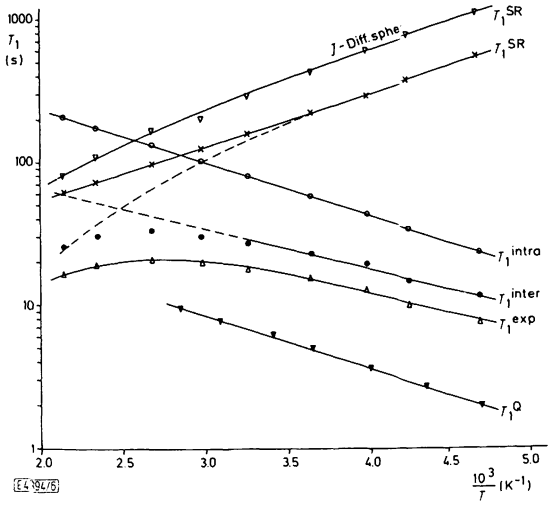

Fig. 6
Longitudinal relaxation times (T_1) of the protons in NH_3 (T_1^{exp}) and ND_3 (T_1^{Q}) at 50 MPa as function of the reciprocal temperature.
○ T_1^{intra} intramolecular dipole-dipole relaxation rates of the protons in NH_3.
● T_1^{inter} intermolecular dipole-dipole relaxation rates of the protons in NH_3.
× T_1^{SR} spin rotation contribution to the experimental proton T_1.
▽ T_1^{SR} calculated from the spherical J-diffusion model (15).
Details of the separation procedure for the different contributions to the experimental proton T_1 are given in the theoretical section [Eqs. (4), (5), and (6)]

positions in the molecular frame of the corresponding vectors characterizing the interaction in question have been neglected. Since Eq. (5) has been experimentally verified in the case of nitrogen 14 in NH_3 and ND_3, where $\tau^{(2)}_{\theta,\mathrm{eff}} = \tau^{(2,0)}$ it seems to be more appropriate to transform the spherical components instead of the effective correlation times. At pressures

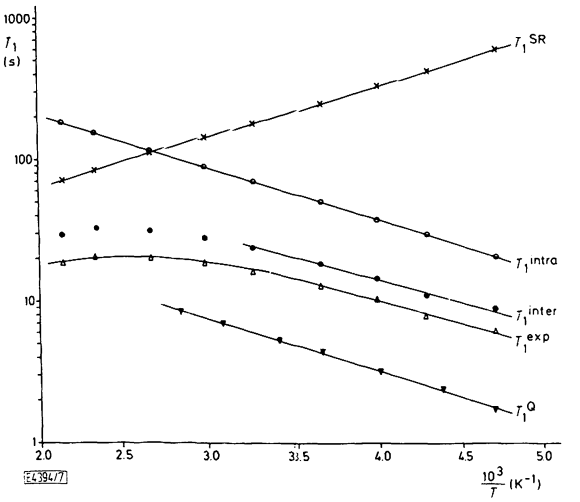

Fig. 7
Longitudinal relaxation times (T_1) of the protons in NH_3 (T_1^{exp}) and ND_3 (T_1^{Q}) at 150 MPa as function of the reciprocal temperature.
○ T_1^{intra} intramolecular dipole-dipole relaxation rates of the protons in NH_3.
● T_1^{inter} intermolecular dipole-dipole relaxation rates of the protons in NH_3.
× T_1^{SR} spin rotation contribution to the experimental proton T_1.
Details of the separation procedure for the different contributions to the experimental proton T_1 are given in the theoretical section (Eqs. (4), (5), and (6)]

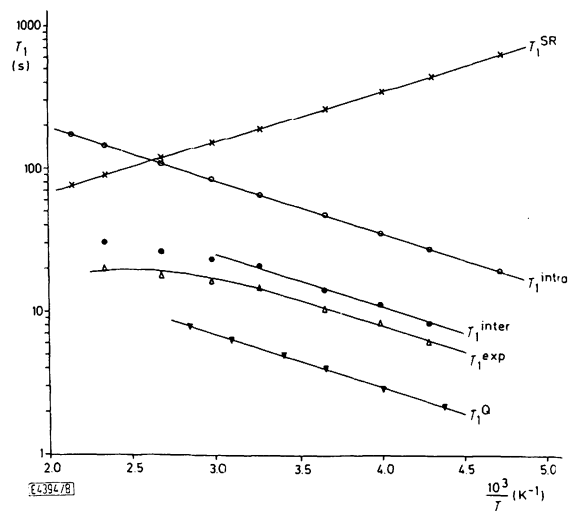

Fig. 8
Longitudinal relaxation times (T_1) of the protons in NH_3 (T_1^{exp}) and ND_3 (T_1^{Q}) at 250 MPa as function of the reciprocal temperature.
○ T_1^{intra} intramolecular dipole-dipole relaxation rates of the protons in NH_3.
● T_1^{inter} intermolecular dipole-dipole relaxation rates of the protons in NH_3.
× T_1^{SR} spin rotation contribution to the experimental proton T_1.
Details of the separation procedure for the different contributions to the experimental proton T_1 are given in the theoretical section [Eqs. (4), (5), and (6)]

above saturation pressure only proton and deuteron T_1-measurements are available. It is therefore impossible to evaluate the spherical components $\tau^{(l,m)}_{\theta}$ of the effective orientational correlation times.

From the data presented here, it cannot be decided which motional model should be applied for the description of the dynamic behaviour of liquid ammonia. However, only at the highest temperatures measured ($T \gg 350$ K) the calculated effective correlation times $\tau_{\theta,\mathrm{eff}}^{(2)*}$ leave the regime where all models merge into the small-step diffusion limit [27]. Because no independent determination of τ_{θ}^{*} is possible with our measurements, no unambiguous decision for one of the different models can be made. One can only exclude the Ivanov-model [27, 29] since the lowest $\tau_{\theta,\mathrm{eff}}^{(2)*}$ estimated fall below the minimum value possible in this model. In the low temperature region the small-step diffusion model should provide a reliable description and thus Eq. (6) was used to compute the angular momentum correlation times τ_J; they are also given in Table 3.

Application of high pressure is seen to influence both correlation times in an opposite way. While the orientational correlation time $\tau_{\theta,\mathrm{eff}}^{(2)}$ increases with increasing pressure by $\sim 30\%$, the angular momentum correlation time τ_J decreases over the same pressure range by the same amount. This behaviour only reflects the assumed relationship $\tau_\theta \cdot \tau_J = \mathrm{const}$ for an isotherm and is certainly in accord with small-step diffusive motion. The intermolecular relaxation rate is again the dominating relaxation mechanism amounting from $\sim 67\%$ at low pressures to $\sim 76\%$ at the highest pressure. Thus the intermolecular dipole-dipole relaxation becomes more efficient with increasing pressure. This is to be expected since increasing density should increase the average number of next neighbours in a liquid and might probably also decrease the distance r_{12} between two protons on different molecules thus enhancing the intermolecular dipole-dipole interaction. Increasing temperature causes the intermolecular relaxation rate to decrease. At the highest temperatures our separation procedure leads to an apparent increase for the efficiency of the intermolecular dipole-dipole interaction which is physically unacceptable and certainly an indication that the separation procedure applied fails at high temperatures and therefore small-step diffusion is no longer applicable. Assuming T_1^{inter} to increase linearly on a semilog $1/T$-plot one can conclude, that the spin-rotation contribution to the experimental relaxation rate becomes even more effective than is described by Eq. (3). It is probable that the J-diffusion model [15] predicts the true temperatu dependence as indicated by a computation of T_1^{SR} with anexpression given in Ref. [15], regarding for simplicity NH_3 s a spherical molecule. However the absolute values of T_1^{SR} re much to high to remove the apparent maximum in e T_1^{inter} versus T^{-1} isobares. In order to decide this quion it would be necessary to measure the proton spin-latce relaxation times in NH_3 at higher temperatures where thspin-rotation mechanism becomes even more dominating. T high temperatures necessary cannot be obtained with e variable temperature unit of our present spectrometer.

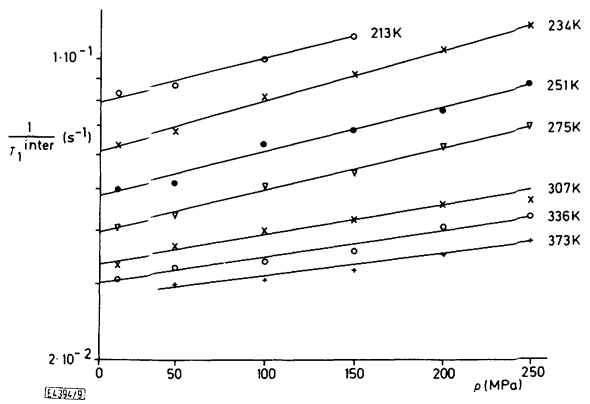

Fig. 9
Pressure dependece of the intermolecular dipole-dipole relaxation rates in NH_3

The dynamic processes underlying the intra- and intermolecular relaxaion mechanisms are normally considered as thermally activaed. The corresponding activation energies and activation vlumes can be calculated from the respective semilog plots of τ_θ versus temperature and pressure (Figs. 5 and 9). Thesc parameters are collected in Table 4. All activation energis derived are significantly higher than kT, showing that the reorientation processes in liquid ammonia can be described s activated processes. It is generally assumed that the intramdecular dipole-dipole relaxation process is determined by tle rotatoric reorientation of the molecules. The activation energy at constant pressure of 7 kJ · mol^{-1} for this process is to e compared with the corresponding results

Table 4
Activation energies and activation volumes calculated from the isobars, isochor or isotherms of the relaxation rates

Activation energies

$(\Delta E_a^{\mathrm{intra}})_{p=\mathrm{const.}}$ [kJ · mol^{-1}]		7.0 ± 0.5				
$(\Delta E_a^{\mathrm{inter}})_{p=\mathrm{const.}}$ [kJ · mol^{-1}]		6.0 ± 1.0				
ρ [g · cm^{-3}]		0.684	0.837	0.193		
$(\Delta E_a^{\mathrm{intra}})_{\rho=\mathrm{const.}}$ [kJ · mol^{-1}]		5.5 ± 0.5	5.7 ± 0.5	5.[illegible] ± 0.5		

Activation volumes

T [K]	213	234	251	275	307	336
$\Delta V_{\mathrm{intra}}^{*}$ [cm^3 · mol^{-1}]	1.9 ± 0.6	2.0 ± 0.6	2.2 ± 0.6	2.[illegible] ± 0.6	2.6 ± 0.6	3.0 ± 0.6
$\Delta V_{\mathrm{inter}}^{*}$ [cm^3 · mol^{-1}]	4.7 ± 1.0	5.0 ± 1.0	5.2 ± 1.0	5.[illegible] ± 1.0	4.2 ± 1.0	4.4 ± 1.0

for water, where values around 14 kJ · mol^{-1} are derived [30] and for liquid hydrogensulfide [31] which yields ~3 kJ · mol^{-1}. The comparison of these three molecules of similar size and moment of inertia shows that in liquid ammonia the hydrogen bonding between next neighbors hinders the reorientational process. This explanation lends further support from the activation energies at constant density of ~6 kJ · mol^{-1}. The ratio of the two activation energies is ~0.8 in ammonia, while in normal liquids a ratio around 0.5 is found [32]. The intermolecular relaxation rates are mainly determined by translational processes, the activation energy derived for these processes is also very close to the value found for the rotation of a molecule. This indicates again that identical activated processes which might tentatively be explained as the breaking of a hydrogen bond are responsible for this type of molecular motion.

From the isothermal pressure dependence of the different relaxation processes the activation volume ΔV^* defined by

$$\Delta V^* = -RT\left(\frac{\partial \ln T_1}{\partial P}\right)_T$$

can be derived. ΔV^* is generally taken as a qualitative measure of the space required by a molecule to reorient or translate to a new position in the cage of its next neighbours. ΔV^* for the rotational processes increases continuously with rising temperature. The same behaviour would be expected for the intermolecular term and the apparent decrease of $\Delta V^*_{\text{inter}}$ found for the 307 K, 336 K, and 373 K isotherms might, as mentioned in the previous section, be an artefact of our separation procedure. All activation volumes derived for the intramolecular relaxation rate are significantly smaller than the corresponding values for the intermolecular term, thus indicating that the translational diffusion is slowed down faster with increasing density than the rotational diffusion.

Conclusions

In the temperature range below 350 K the small-step diffusion model seems to provide an adequate description of the dynamics of liquid ammonia. Due to the limited temperature range of the present investigation no decision can be made about the appropriate model for the molecular mobility at higher temperatures. Compared to water at room temperature the reorientational correlation times found in liquid ammonia are more than an order of magnitude shorter. Furthermore the temperature dependence of $\tau^{(2)}_{\theta,\text{eff}}$ in ammonia is much smaller than in water. While in supercooled D_2O $\tau^{(2)}_{\theta,\text{eff}}$ increases between 200 K and 300 K by three orders of magnitude [30, 35], the corresponding change in liquid ND_3 is only a factor of 5. This indicates a much weaker intermolecular interaction than derived for the strongly hydrogen-bonded water. That some hydrogen bonding must exist in liquid ammonia becomes however evident from a comparison between the activation parameters derived for the rotational and translational diffusion in NH_3 and H_2S. In the latter liquid the activation energies for the rotational and translational motion differ significantly [31] while in NH_3 the isobaric and isochoric activation energies for the rotation as well as the corresponding energy for translational diffusion are very similar. Further evidence for this conclusion can be drawn from the low value of the deuteron QCC of 210 kHz derived for liquid ND_3 as compared to the result observed in the gas of 282 kHz resp. the solid of 156 kHz. An increase of 80% for the QCC in ND_3 in going from the solid state to the gas is comparable to the increase of the QCC of D_2O from ice to water vapour of +66%. In non hydrogen-bonded liquids as for instance D_2S [36, 37] this change amounts only to −4%.

The radial distribution function of liquid NH_3 derived from X-ray scattering [2] reveals approximately 12 next neighbours around a central molecule. This is in marked contrast to the result found in liquid water where the approximately tetrahedral symmetry of the ice crystal appears to be locally preserved and the central molecule is only surrounded by ~4.4 next neighbours. Considering these observations, it is thus not surprising that the reorientational correlation times $\tau^{(2)}_{\theta,\text{eff}}$ in liquid ammonia increase continuously with pressure in the pressure range studied and reveal none of the anomalies observed at low temperatures and pressures in water.

The technical support by Mr. R. Knott and Mr. S. Heyn is gratefully acknowledged.

This work was supported by grants from the Deutsche Forschungsgemeinschaft and the Fonds der Chemischen Industrie.

References

[1] C. N. R. Rao, in: F. Franks, ed., Water – A Comprehensive Treatise, Vol. 1, p. 93ff., Plenum Press, New York 1972.
[2] A. H. Narten, J. Chem. Phys. *66*, 3117 (1977).
[3] J. L. Carolan and T. A. Scott, J. Magn. Reson. *2*, 243 (1970).
[4] W. M. Litchman and M. Alei, Jr., J. Chem. Phys. *56*, 5818 (1972).
[5] W. G. Schneider, Symposium on Hydrogen Bonding, Ljubljana 1957.
[6] J. G. Powles and M. Rhodes, Mol. Phys. *12*, 399 (1967).
[7] D. W. G. Smith and J. G. Powles, Mol. Phys. *10*, 451 (1966).
[8] P. W. Atkins, A. Loewenstein, and Y. Margalit, Mol. Phys. *17*, 329 (1969).
[9] J. G. Powles, M. Rhodes, and J. H. Strange, Mol. Phys. *11*, 515 (1966).
[10] G. Völkel, E. Lang, and H.-D. Lüdemann, Ber. Bunsenges. Phys. Chem. *83*, 722 (1979).
[11] A. Abragam, The Principles of Nuclear Magnetism, Oxford University Press 1961.
[12] H. W. Spiess, in: P. Diehl, E. Fluck, R. Kosfeld, eds., NMR-Basic Principles and Progress, Vol. 15, p. 55ff., Springer Verlag, Berlin 1978.
[13] W. A. Steele, in: I. Prigogine and S. A. Rice, eds., Advances in Chemical Physics, Vol. 34, p. 1ff., Wiley, New York 1976.
[14] M. D. Zeidler, Ber. Bunsenges. Phys. Chem. *75*, 229 (1971).
[15] R. E. D. McClung, Advances in Molecular Relaxation and Interaction Processes *10*, 83 (1977).
[16] P. S. Hubbard, Phys. Rev. *131*, 275 (1963).
[17] H. C. Torrey, Phys. Rev. *92*, 962 (1953).
[18] J. F. Harmon and B. H. Muller, Phys. Rev. *182*, 400 (1969).
[19] B. H. Muller, Phys. Lett. *22*, 123 (1966).
[20] J. F. Harmon, J. Magn. Reson. *31*, 411 (1978).
[21] R. L. Cook and F. C. DeLucia, Am. J. Phys. *39*, 1433 (1971).
[22] C. H. Wang, J. Magn. Reson. *9*, 75 (1973).
[23] R. M. Garvey, F. C. DeLucia, and J. W. Cederberg, Mol. Phys. *31*, 265 (1976).

[24] Landolt-Börnstein, New series, K.-H. Hellwege, A. M. Hellwege, eds., Springer Verlag, Berlin 1974, Vol. II/6, p. 413.
[25] P. S. Hubbard, Phys. Rev. *131*, 1155 (1963).
[26] D. W. Sawyer and J. G. Powles, Mol. Phys. *21*, 83 (1971).
[27] J. G. Powles and G. Rickayzen, Mol. Phys. *33*, 1207 (1977).
[28] W. T. Huntress, Jr., in: J. S. Waugh, ed., Advances in Magnetic Resonance, Vol. 4, p. 1ff., Academic Press, New York 1970.
[29] E. N. Ivanov, Soviet Phys. JETP *18*, 1041 (1964).
[30] E. Lang and H.-D. Lüdemann, J. Chem. Phys. *67*, 718 (1977).
[31] J. Hauer, Diplomarbeit, Universität Regensburg 1978.
[32] J. Jonas, T. DeFries, and D. J. Wilbur, J. Chem. Phys. *65*, 583 (1976).
[33] E. Lang and H.-D. Lüdemann, to be published.
[34] F. C. DeLucia and J. W. Cederberg, J. Mol. Spectrosc. *40*, 52 (1971).
[35] D. E. O'Reilly and J. H. Eraker, J. Chem. Phys. *52*, 2407 (1970).

(Eingegangen am 27. Juli 1979, E 4394
endgültige Fassung am 18. August 1979)